Energy Conversion and Management: X 22 (2024) 100530

Contents lists available at ScienceDirect

Energy Conversion and Management: X

journal homepage: www.sciencedirect.com/journal/energy-conversion-and-management-x

Optimization and assessment of solar-assisted cooling systems: A multicriteria framework and comparative study

Dana Alghool [a], Reem Khir [b], Mohamed Haouari [a,*]

[a] Department of Mechanical and Industrial Engineering, Qatar University, Doha, Qatar
[b] School of Industrial Engineering, Purdue University, West Lafayette, IN, United States

ARTICLE INFO

Keywords:
Solar cooling systems
System modeling
Optimization
Multiple criteria decision analysis

ABSTRACT

In the current context of global warming, where district cooling systems are increasingly burdening power grids worldwide, it is important to design and operate alternative systems that are not only environmentally friendly, but also cost effective for sustainable energy transition. This paper investigates the potential of two, previously unexplored, solar cooling systems while considering economic and environmental criteria: a Solar Thermal and Electrical Cooling System (STECS) that relies solely on solar energy, offering a significant environmental advantage, and a Hybrid Solar Cooling System (HSCS) that combines a compression chiller and an absorption chiller for improved efficiency. First, novel Mixed-Integer Linear Programming models are proposed to aid in generating cost-effective designs and operations for each of STECS and HSCS. Second, the Technique for Order Preference by Similarity to Ideal Solution (TOPSIS) is adapted to evaluate both systems and benchmark them against conventional cooling systems previously studied in the literature. The proposed framework allows decision makers to assess the potential of these systems using three criteria; namely, cost, carbon dioxide emissions, and noise levels, which are crucial for ensuring the social acceptance of district cooling technologies worldwide. A computational study is presented to show the practical relevance of the proposed framework using real-demand data obtained from an educational district in the State of Qatar. Results show that the integration of solar energy into conventional cooling systems has the potential to significantly reduce the annual total net cost by 61%, CO_2 emissions by 60%, and noise levels by 53%, on average. Additionally, the benchmark results demonstrate that the zero-carbon dioxide emissions solar cooling system achieves the highest overall performance score when all criteria are considered together.

1. Introduction

The presence of Greenhouse Gases (GHG) in the atmosphere has increased by around 47% over the last decade, escalating further global warming while increasing demand for cooling services [33]. Nowadays, cooling demand is mainly satisfied by conventional cooling systems such as split air conditioners, window air conditioners, and district cooling systems. These systems consume excessive electricity for their operations, thus, putting significant stress on the power grid globally. Renewable cooling technologies offer a climate-friendly alternative for reducing conventional energy use and their resulting GHG emissions. Their environmental benefits depend on various design and operational factors that consequently influence their cost effectiveness and ultimately impact their market adoption. The current literature on comparing the potential of different cooling systems is primarily focused on cost-related metrics, except the work done by Fumo et al. [14] and Otanicar et al. [19] that provides an analytical approach to independently evaluate the economic and environmental benefits of different thermal cooling systems. To the best of knowledge, this paper is the first to propose a multi-criteria assessment framework that provides planners and decision-makers with a holistic understanding of the economic and environmental benefits of different solar cooling systems. It includes (1) an optimization module that is responsible for generating cost-effective design and operations of a selected solar cooling system and (2) a multi-criteria decision analysis tool that enables finding trade-offs between economic and environmental benefits simultaneously rather than independently, hence, providing-decision makers with a comprehensive view of alternatives to select the one that best matches their specific requirements.

The concept of integrating renewable energy in the form of photovoltaic (PV) panels and solar collectors into conventional cooling systems, known as solar-assisted cooling systems, has been addressed in recent research. A detailed survey is given in Section 2. This paper adds

* Corresponding author.

https://doi.org/10.1016/j.ecmx.2024.100530

Available online 17 January 2024

Nomenclature

Abbreviation

Greenhouse Gases GHG
Photovoltaic PV
Solar Thermal and Electrical Cooling System STECS
Hybrid Solar Cooling System HSCS
Baseline Conventional Cooling System BCCS
Solar Electric Cooling System SECS
Mixed Integer Linear Programming MILP
Technique for Order of Preference by Similarity to Ideal Solution TOPSIS
Thermal Energy Storage TES
TraNsient SYstem Simulation TRNSYS
Coefficient of Performance COP
Cooling, Heating, and Power CHP
Annualized Operational Cost AOC
Annualized Investment Cost AIC
Qatar University QU

to the body of literature in this area by comparing the economic and environmental benefits of two types of solar-assisted cooling systems that have not been studied yet in the literature. The first system is a Solar Thermal and Electricity Cooling System, henceforth referred to as STECS. This system can be classified as a zero-carbon emissions system from an operational standpoint. It completely depends on solar energy for its operation; the required electricity and thermal energy for the operations of its chillers are generated from PV panels and solar collectors, respectively. The second system is a Hybrid Solar Cooling System, henceforth referred to as HSCS. This system is designed to operate both an electricity-driven compression chiller and a thermally-driven absorption chiller to meet the cooling demand. It uses PV panels and solar collectors to produce respectively the electricity and thermal energy needed to operate the system. Unlike SETCS, this system can use electricity from the grid for operations. The STECS and HSCS are allowed the use of net metering options that enable selling excess energy back to the grid, thus, allowing users to generate revenues as a way to incentivize the use of renewables. Such variations in systems' components dictate a need for system-specific solution approaches to better capture each system's dynamics and operational realities.

To this end, this paper makes the following contributions:

- It introduces the design of two efficient integrated solar cooling systems that have not been studied before, namely a Solar Thermal and Electrical Cooling System (STECS) and a Hybrid Solar Cooling System (HSCS) while considering three important criteria: annual total net cost, CO_2 emissions, and noise level. To achieve this, this paper develops computationally-tractable mathematical optimization models for the design and operations of a STECS and a HSCS using Mixed-Integer Linear Programming (MILP). The objective of the optimization models is to find the best system configuration that minimizes total annualized investment and operational costs while maximizing the revenue generated from selling excess energy back to the grid. To demonstrate the computational effectiveness of these models, this paper utilizes real data from an educational district in Qatar.
- It performs a comparative analysis of four optimized solar cooling systems–two drawn from existing literature and two introduced within this paper namely, a Baseline Conventional Cooling System (BCCS) [3], a Solar Electric Cooling System (SECS) [3], STECS, and HSCS—, to determine the most effective system considering all criteria simultaneously. To evaluate all criteria simultaneously, this paper applies a multi-criteria assessment tool, namely, the Technique for Order of Preference by Similarity to Ideal Solution (TOPSIS) method coupled with Shannon's entropy method, to aid decision-makers in evaluating systems that trade-off annual total net system cost, CO_2 emissions level, and operational noise level.

Fig. 1 depicts a flowchart illustrating the step-by-step methodology employed in addressing the novelty of this paper.

2. Literature Review

This section presents a summary of related work. It first discusses research that focused mainly on using simulation and/or optimization approaches to design solar-assisted cooling systems. Then, it discusses efforts that are aimed at comparing the potential of different solar-assisted cooling systems. Finally, it highlights the novelty of this work in relation to the existing literature. This paper refers the reader to Section 1 of the supplementary material that has the detailed description of the contribution and outcomes of each related work to keep the length of the paper at a reasonable length.

2.1. Simulation and Optimization Methods for Solar Assisted Cooling Systems

The design of solar-assisted cooling systems from a simulation lens has gained ample attention in the literature during the last decade (see for example Abusaibaa et al. [2], Khan et al. [16], Sokhansefat et al. [25], and Soussi et al. [27]), where these work are the most recent in that area. The cooling systems structure investigated in current research primarily included absorption chillers, solar collectors, and cold-water thermal energy storage (TES) while using TraNsient SYstem Simulation (TRNSYS) software to analyze and assess their designs and operational strategies. Key investigated decisions include determining the absorption chiller, storage tank, and auxiliary boiler capacities, solar collector area and orientations, and chiller coefficient of performance (COP). Another stream of research used an optimization approach to design cooling systems either by using a simulation-based optimization framework (see for example Bilardo et al. [8], Calise et al. [11], where these work are the most recent in that area) or a standalone optimization procedure (see for example, Al-Noaimi et al. [5], Gang et al. [15], and Reda et al. [23], Alghool et al. [3] and Khir and Haouari [17]). In their paper, Alghool et al. [3] developed a MILP model to optimize the design and operation of a solar electric cooling system and a conventional cooling system. Both models addressed the optimal design which was reflected in specifying the capacity, investment cost, and efficiency of each system component. Both models also determined the optimal operating policies which were reflected in specifying the quantities of cold thermal energy produced and stored and quantities of electricity produced and sold. Abdollahi and Sayyaadi [1] and Brandoni and Renzi [9] have studied the existence of both absorption chiller and compression as a part of cooling, heating, and power (CHP) generation systems from an optimization perspective. Nevertheless, their developed systems are not classified as hybrid systems since the compression chiller is used as an auxiliary chiller, and the chillers are a part of a larger system. Other efforts focused on studying and analyzing the thermodynamics of hybrid solar cooling systems (see for example Wang et al. [31], Zeng et al. [34], and Zhang et al. [35]), where these work are the most recent in that area. Both absorption and compression chiller systems were integrated, where the output of the absorption sub-system is the input to the compression sub-system. These studies differ from this work in terms of components, the type of renewable energy employed, and optimization objective(s).

2.2. Comparative studies of Solar Assisted Cooling Systems

Comparing different types of cooling systems has gained ample attention recently, mainly to better assess the feasibility and

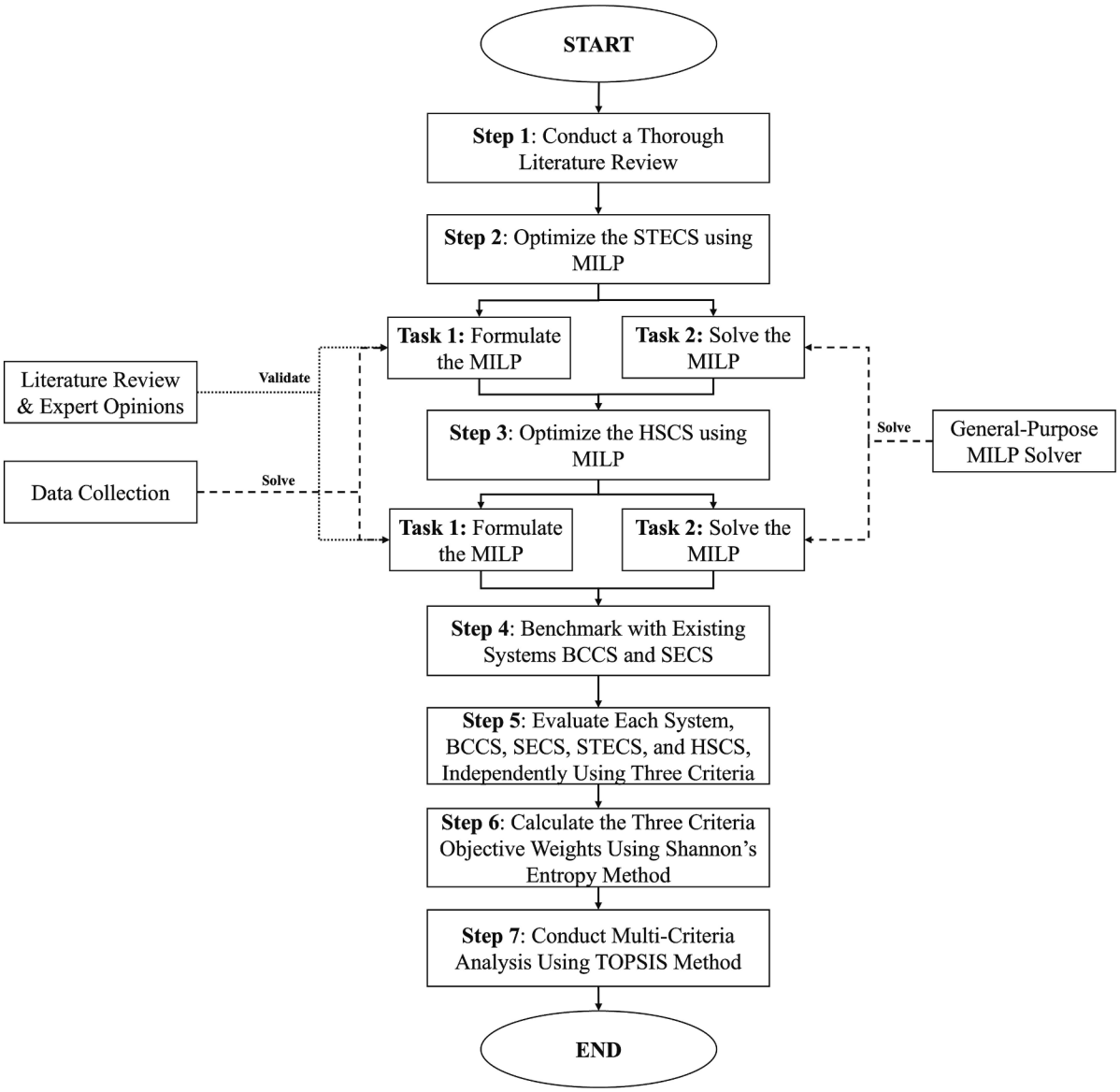

Fig. 1. The methodology of this paper.

effectiveness of different cooling technologies. Ayadi and Al-Dahidi [7] and Brumana et al. [10], Eicker et al. [12], Noro and Lazzarin [18], and Shirazi et al. [24] carried out comparison studies between different types of solar cooling systems that were developed and simulated on TRNSYS software.Al-Ugla et al. [6], Fumo et al. [14], Otanicar et al. [19], Papoutsis et al. [21], and Porumb et al. [22] carried out comparison studies between different types of solar cooling systems without specifying the methods used to develop the systems. The different assessment criteria used in each study are highlighted in Table 1.

To the best of knowledge, this paper is the first to (1) introduce MILP optimization models to optimize the design and operating policies of the STECS and HSCS and (2) perform a comparison study between various types of mathematically optimized solar-assisted cooling systems using optimization and a multi-criteria assessment framework that takes into account important economic and environmental considerations.

3. Solar-assisted Cooling Systems

This section describes the two cooling systems of interest in terms of setup and primary components. It introduces mathematical notation that will be used later in the problem formulation. The modeling considers a time horizon of a year with 1-h time discretization; that is, this paper investigates designs that optimize hourly operations to capture real-life system behavior better.

3.1. Solar Thermal and Electrical Cooling System (STECS)

The STECS consists of eight main components, namely, absorption chiller, ice chiller, auxiliary electric boiler, ice TES, cold-water TES, hot-water TES, solar collectors, and PV panels. It is designed to operate with nearly zero-carbon dioxide emissions. Fig. 2 illustrates the system's components and highlights its corresponding energy flows in the form of cold thermal energy, hot thermal energy, and electricity; the arrows indicate the flow direction and are tracked over time for each period t. This paper describes the process in what follows; notation in the parenthesis refers to the mathematical notation used later in problem modeling. The operation starts with solar collectors generating hot thermal energy (L_t^{SC}), and PV panels generating electricity (L_t^{PV}) using sun radiation (G_t). The electricity generated by the PV panels can be used to power the ice chiller (L_t^{PVI}), and/or the auxiliary electric boiler (L_t^{PVB}). If it exceeds the ice chiller and auxiliary electric boiler needs, the

Table 1
Assessment criteria of different study.

Study	Economic Criterion	Environmental Criterion	Noise Criterion
Otanicar et al. (2012)	✓	✓	x
Fumo et al. (2012)	✓	✓	x
Eicker et al. (2014)	✓	x	x
Noro and Lazzarin (2014)	✓	x	x
Shirazi et al. (2016)	✓	x	x
Porumb et al. (2016)	✓	x	x
Al-Ugla et al. (2016)	✓	x	x
Papoutsis et al. (2017)	✓	x	x
Ayadi and Al-Dahidi (2019)	✓	x	x
Brumana et al. (2021)	✓	x	x
This Paper	✓	✓	✓

surplus electricity generated is sold to the grid ($L_t^{\overline{PV}}$). The hot thermal energy generated by solar collectors can be used to power the absorption chiller directly (F_t^{InA}), or get stored at the hot-water TES (M_t) to generate energy (D_t^{HWT}) that can be used later to power the absorption chiller. The absorption chiller can be powered by the hot thermal energy generated from the solar collectors (F_t^{InA}), the auxiliary electric boiler (B_t^{Ch}), and/or the hot-water TES (D_t^{HWT}). The surplus hot thermal energy generated by the auxiliary boiler (B_t^{HWT}) is stored at the hot-water TES. The cold thermal energy produced by the absorption chiller (F_t^{Oab}) can be used to meet the cooling demand directly (S_t^{CW}) or get stored at the cold-water TES (E_t) to satisfy the cooling demand (D_t^{CWT}) when needed. The ice chiller uses the electricity from PV panels to produce the energy needed to cool the water and turn it into ice (P_t) which is stored at the ice TES. The ice chiller supplies the ice TES with the energy required to maintain the built-up ice at the ice TES (H_t). The built-up ice at the ice TES gets melted, and the resulting cold thermal energy can be used to satisfy the

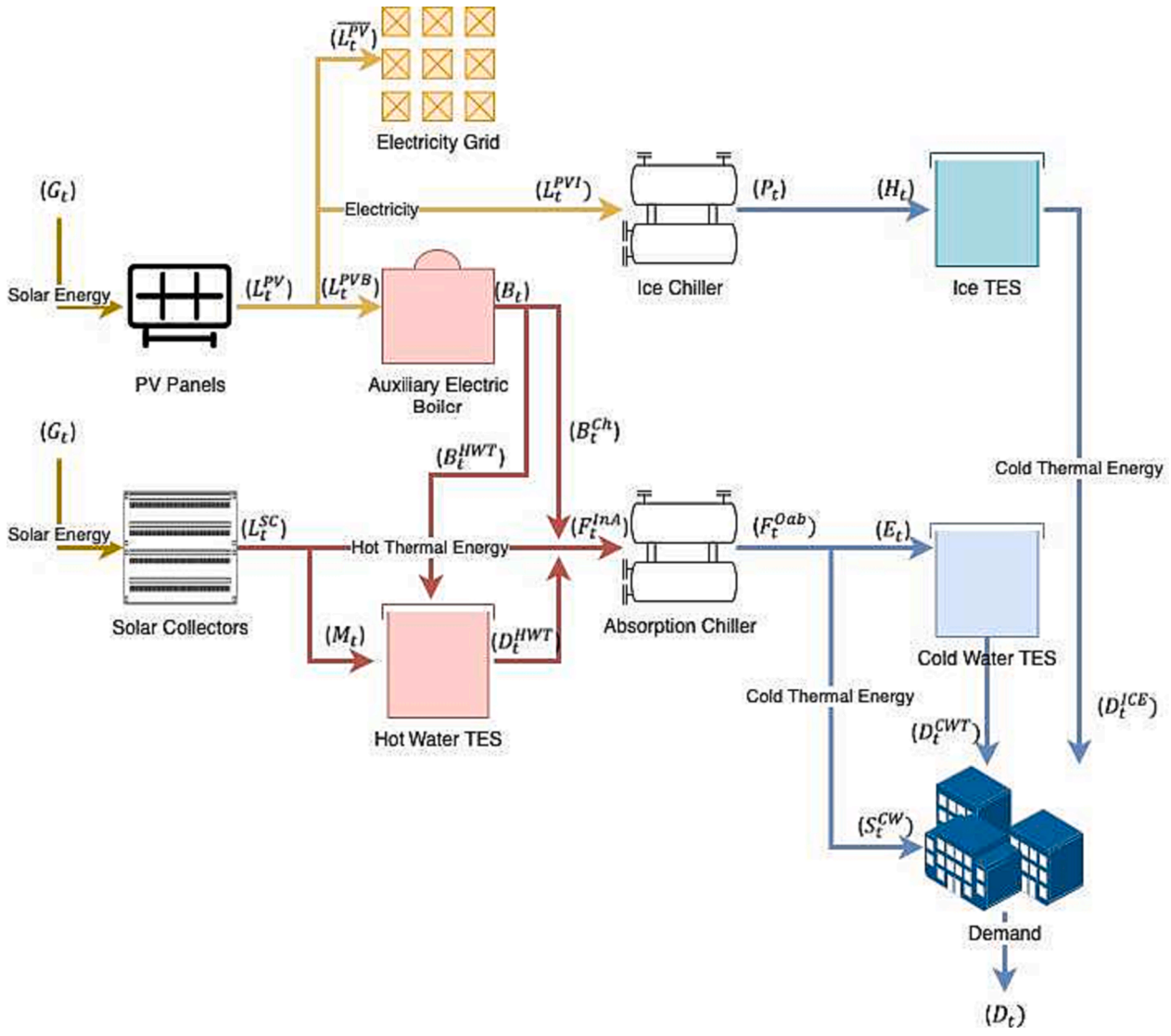

Fig. 2. An illustration of the STECS components.

cooling demand (D_t^{ICE}) when needed.

3.2. Hybrid Solar Cooling System (HSCS)

Unlike the STECS, the HSCS operates a compression chiller and does not include an ice chiller or an ice TES, resulting in different system structures and dynamics. This paper uses similar notations to those used to describe the STECS and introduce additional notations where needed to capture the differences in the system's dynamics. Fig. 3 illustrates the system's components and energy flow in the form of cold and hot thermal energy and electricity through the system's components; the arrows indicate the flow direction and are tracked over time for each period t. This paper describes the process in what follows; notation in the parenthesis refers to mathematical notations used later in problem modeling. The system's operation starts with PV panels and solar collectors, denoted by G_t. Using sun radiation, PV panels generate electricity (L_t^{PV}) while solar collectors generate hot thermal energy (L_t^{SC}). The electricity generated by PV panels can be used to power the auxiliary electric boiler (L_t^{PVB}). If the generated electricity by PV panels exceeds the auxiliary electric boiler needs, then the surplus electricity generated is sold to the grid ($L_t^{\overline{PV}}$). The grid can be used to power the compression chiller (F_t^{InC}) and/or the auxiliary electric boiler (K_t^B). The hot thermal energy generated by the solar collectors can be used to power the absorption chiller directly (F_t^{InA}) or get stored at the hot-water TES (M_t) to be used to satisfy the cooling demand (D_t^{HWT}) when needed. The absorption chiller can be powered by the hot thermal energy generated from the solar collectors (F_t^{InA}), the auxiliary electric boiler (B_t^{Ch}), and/or the hot-water TES (D_t^{HWT}). The surplus hot thermal energy generated by the auxiliary boiler (B_t^{HWT}) can be stored at the hot-water TES. The compression chiller, when used, is powered with electricity (F_t^{InC}) generated from the grid. The cold thermal energy produced by the absorption chiller (F_t^{Oab}), the compression chiller (F_t^{Oco}), or both (F_t^{O}) can be used to meet the cooling demand directly (S_t^{CW}), or get stored at the cold-water TES (E_t) to satisfy the cooling demand (D_t^{CWT}) when needed.

This paper proposes a deterministic mathematical model for both STECS and HSCS to find the optimal design and hourly operating policies given an expected annual hourly demand. The goal is to find the optimal capacity of each system component as well as production and storage strategies that minimizes the total system costs while maximizing generated revenues. Formal definitions of the decision variables and system's constraints of the two systems are given in Section 4.

4. Mathematical Modelling

This paper now presents the MILP formulations for the STECS. The MILP formulation for the HSCS is quite similar to the one developed for STECS with minor differences. The full description of Model HSCS is included in Section 3 in the supplementary material. The goal is to find the optimal design and operating policies of system's components with the objective of minimizing the total system's annualized cost over its lifetime and maximizing revenues generated from selling excess energy back to the grid. Key assumptions in the modeling are that (i) each

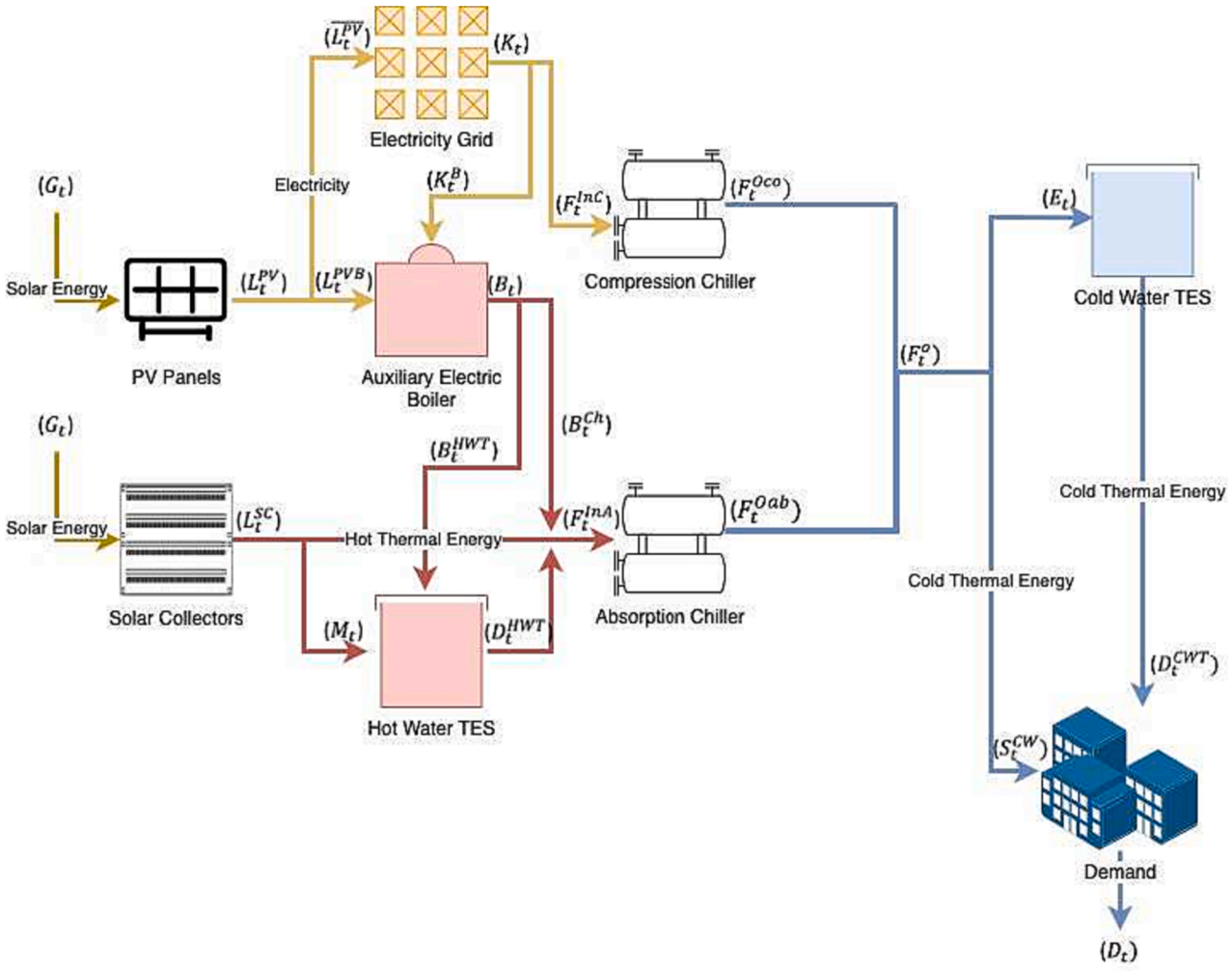

Fig. 3. An illustration of the HSCS components.

system operates in a steady-state mode, (ii) solar collectors and PV panels efficiencies are constant and known in advance, (iii) a chiller of any type operates given a pre-defined COP, and its COP varies with the outdoor temperature, and (iv) TES of any type operates using a pre-defined efficiency level that is known in advance.

4.1. Decision Variables

The system's variables were described earlier in Section 3, and they correspond to various components' capacity, efficiency, investment cost, and variable cost. This paper refers the reader to Section 2 in the supplementary material for a complete list of the notation and definitions.

The decision variables include design decisions as well as operational decisions. The design decisions are related to (i) determining whether a component is included in the system, and (ii) determining the capacity of each component, if present. The operational decisions are defined for every operating period (hour). They are related to determining the quantities of (i) hot thermal energy and electricity generated from solar collectors and PV panels, (ii) cold thermal energy produced by the absorption chiller and ice chiller, (iii) electricity generated by the grid and auxiliary boiler, (iv) cold thermal energy or hot thermal energy stored in cold-water and hot-water TES, and (v) energy or electricity exchanged between components. Section 2 in the supplementary material includes a detailed list of decision variables and their definitions.

4.2. Objective Function

The objective is to generate a system design that minimizes system's annual total net costs modeled as

$$\min \quad \rho\Bigg[\sum_{k\in K} FC_k^{Ch} y_k + \sum_{g\in G} FC_g^{Ic} d_g + F^{sc} x_{sc} + F^{PV} x_{PV} + \sum_{h\in H} FC_h^{CW} g_h + \sum_{j\in J} FC_j^{HW} z_j + \sum_{i\in I} FC_i^{Is} c_i + \sum_{q\in Q} FC_q^{HW} w_q\Bigg] + \sum_{t\in T} VC_t^{Ch} F_t^{Oab} + \sum_{t\in T} VC_t^{Ic} P_t + \sum_{t\in T} VC_t^{HW} B_t - \sum_{t\in T} SL_t^{\overline{PV}} \tag{1}$$

The objective function 1 minimizes the difference between the annualized operational and investment costs of the system, denoted henceforth as AOC and AIC, respectively, and the annual revenues obtained from selling surplus PV-generated electricity back to the grid ($SL_t^{\overline{PV}}$). The AOC includes the variable costs of producing cold thermal energy from the absorption chiller ($VC_t^{Ch}F_t^{Oab}$), energy from the ice chiller ($VC_t^{Ic}P_t$), and hot thermal energy from the auxiliary electric boiler ($VC_t^{HW}B_t$). The AIC includes the investment costs of an absorption chiller ($FC_k^{Ch}y_k$), an ice chiller ($FC_g^{Ic}d_g$), solar collectors ($F^{sc}x_{sc}$), PV panels ($F^{PV}x_{PV}$), a cold-water TES ($FC_h^{CW}g_h$), a hot-water TES ($FC_j^{HW}z_j$), an ice TES ($FC_i^{Is}c_i$), and an auxiliary electric boiler ($FC_q^{HW}w_q$). All investment costs are presented as annualized equivalence costs using a discount factor ρ. In the computational experiments, this paper sets ρ to equal to $\frac{i(i+1)^n}{(1+i)^n-1}$, where n is the component's life time and i is the interest rate.

4.3. Constraints

This section describes capacity, flow balance, and demand constraints that need to be accounted for when designing the system. It first provides a high-level description of each system's constraints, followed by their corresponding MILP formulation.

Capacity Constraints. Constraint (2) ensures that a single absorption chiller is installed with capacity $k \in K$. Similarly, constraint (3) ensures that a single ice chiller is installed with capacity $g \in G$ while constraint (4) ensures that an ice TES is installed with capacity $i \in I$.

$$\sum_{k\in K} y_k = 1, \tag{2}$$

$$\sum_{g\in G} d_g = 1, \tag{3}$$

$$\sum_{i\in I} c_i = 1, \tag{4}$$

Constraints (5)–(7) are optional capacity selection constraints for the cold-water TES, hot-water TES, and the auxiliary electric boiler respectively, if present.

$$\sum_{h\in H} g_h \leqslant 1, \tag{5}$$

$$\sum_{j\in J} z_j \leqslant 1, \tag{6}$$

$$\sum_{q\in Q} w_q \leqslant 1, \tag{7}$$

Constraints (8) ensures that for every period t, the energy produced by the solar collectors is at most equal to the solar energy collected by the installed solar collectors. Similarly, constraints (9) ensure that the energy produced by the PV panels in every period t is at most the available energy collected by the installed PV panels area.

$$L_t^{sc} \leqslant \eta_{sc} G_t x_{sc}, \qquad \forall t \in T \tag{8}$$

$$L_t^{PV} \leqslant \eta_{PV} G_t x_{PV}, \qquad \forall t \in T \tag{9}$$

Constraint (10) ensures that the sum of the installed solar collectors area and the installed PV panels area does not exceed the maximum available area.

$$x_{sc} + x_{PV} \leqslant A \tag{10}$$

Constraints (11) ensure that the cold thermal energy produced from the absorption chiller during every period t does not exceed the selected chiller capacity. Similarly, constraints (12) ensure that the energy produced from the ice chiller during every period t does not exceed the selected chiller capacity.

$$F_t^{Oab} \leqslant \sum_{k\in K} Q_k y_k, \qquad \forall t \in T \tag{11}$$

$$P_t \leqslant \sum_{g\in G} E_g d_g, \qquad \forall t \in T \tag{12}$$

Constraints (13)–(15) ensure that the cold thermal energy inventory level, hot thermal energy inventory level, and the ice energy inventory level do not exceed the selected cold-water TES capacity, hot-water TES capacity, or ice TES capacity, respectively.

$$I_t^{CW} \leqslant \sum_{h\in H} D_h g_h, \qquad \forall t \in T \tag{13}$$

$$I_t^{HW} \leqslant \sum_{j\in J} R_j z_j, \qquad \forall t \in T \tag{14}$$

$$I_t^{Is} \leqslant \sum_{i\in I} I_i c_i, \qquad \forall t \in T \tag{15}$$

Constraints (16) ensure that the hot thermal energy produced from the auxiliary electric boiler does not exceed the selected auxiliary electric boiler capacity.

$$B_t \leqslant \sum_{q \in Q} L_q w_q EFF_q, \qquad \forall t \in T \tag{16}$$

Constraints (17) and (18) introduce the selected absorption chiller COP and ice chiller COP which varies with time, respectively.

$$F_t^{Oab} = \sum_{k \in K} COP_{kt} F_t^{InA} y_k, \qquad \forall t \in T \tag{17}$$

$$P_t \leqslant \sum_{g \in G} COP_{gt} L_t^{PVI} d_g, \qquad \forall t \in T \tag{18}$$

Flow Balance Constraints. Constraints (19)–(21) are the energy balance constraint of the model. Constraints (19) introduce the energy balance constraint for the selected cold-water TES, where the cold thermal energy inventory level of the previous period summed with the cold thermal energy delivered to the cold-water TES at the current period is equal to the cold thermal energy inventory level at the current period summed with the cold thermal energy delivered to satisfy the cooling demand. Constraints (20) and (21) similarly introduce the energy balance constraint for the selected hot-water TES and ice TES, respectively.

$$I_{t-1}^{CW} + \tau E_t = I_t^{CW} + \tau D_t^{CWT}, I_0^{CW} = I_T^{CW}, \qquad \forall t \in T \tag{19}$$

$$I_{t-1}^{HW} + \tau M_t = I_t^{HW} + \tau D_t^{HWT}, I_0^{HW} = I_T^{HW}, \qquad \forall t \in T \tag{20}$$

$$S_t^{CW} + D_t^{CWT} + D_t^{ICE} = D_t, \qquad \forall t \in T \tag{21}$$

Demand Constraints. Constraints (22) enforce the cooling demand to be satisfied from the cold-water TES, the absorption chiller, and/or the ice TES during every period t.

$$S_t^{CW} + E_t = F_t^{Oab}, \qquad \forall t \in T \tag{22}$$

Constraints (23) enforce the cold thermal energy produced from the absorption chiller during every period t to be used to satisfy the cooling demand directly and/or get stored in the cold-water TES. Similarly, constraints (24) enforce the absorption chiller demand for hot thermal energy to be satisfied from hot-water TES, solar collectors, and/or auxiliary electric boiler while constraints (25) enforce the hot thermal energy delivered to the absorption chiller from the hot-water TES is from the auxiliary electric boiler and/or the solar collectors.

$$S_t^{CW} + E_t = F_t^{Oab}, \qquad \forall t \in T \tag{23}$$

$$L_t^{SC} - M_t + B_t^{Ch} + D_t^{HWT} = F_t^{InA}, \qquad \forall t \in T \tag{24}$$

$$M_t + B_t^{HWT} = D_t^{HWT}, \qquad \forall t \in T \tag{25}$$

Constraints (26) enforce that the electricity produced from PV panels during every period t equals the electricity delivered to the auxiliary electric boiler while constraints (27) ensure that the electricity produced from PV panels is used to power the auxiliary electric boiler, the ice chiller, and/or sold to the grid.

$$L_t^{PVB} = B_t, \qquad \forall t \in T \tag{26}$$

$$L_t^{PVB} + L_t^{PVI} + L_t^{\overline{PV}} = L_t^{PV}, \qquad \forall t \in T \tag{27}$$

Constraints (28) enforce that the hot thermal energy produced from the auxiliary electric boiler could satisfy the absorption chiller demand or be stored in the cold-water TES.

$$B_t^{HWT} + B_t^{Ch} = B_t, \qquad \forall t \in T \tag{28}$$

Constraints (29) enforce that the energy delivered to the ice TES is used to maintain the ice state in the ice TES while constraints (30) enforce that the energy produced from the ice chiller equals the energy required to decrease the water temperature and build ice.

$$H_t = F_t^W L, \qquad \forall t \in T \tag{29}$$

$$vP_t = H_t + F_t^W CofT_{in}, \qquad \forall t \in T \tag{30}$$

Non-Negativity and Integrality Constraints. Constraints (31)–(31) are the non-negativity and integrality constraints of the model.

$$y_k, g_h, z_j, w_q, c_i, d_g \in \{0,1\}, \qquad \forall k \in K, h \in H, q \in Q, i \in I, g \in G \tag{31}$$

$$x_{sc}, x_{PV}, F_t^{Oab}, P_t, F_t^{InA}, S_t^{CW}, L_t^{SC} I_t^{CW}, I_t^{HW}, I_t^{Is}, E_t, M_t, H_t, D_t^{CWT}, D_t^{HWT}, B_t, B_t^{Ch}, B_t^{HWT}, L_t^{\overline{PV}} L_t^{PV}, D_t^{ICE}, F_t^W, L_t^{PVI}, L_t^{PVB} \geqslant 0, \qquad \forall t \in T. \tag{32}$$

Objective (1) and constraints (2)–(31) constitute the MILP formulation used to optimize for the STECS model.

5. Data Collection

This paper uses real-life data to assess the operational performance of the proposed models. It obtained data from Qatar University (QU) campus, an educational district in Doha, Qatar. The operations time of QU is from 8 am to 8 pm from Sunday to Thursday. Along with the summer break, there is a winter break from mid-December to mid-January and a week-long Spring break in March. The campus is characterized by very high cooling demand with a peak cooling demand of 6000 tones refrigeration [3]. The data used in the computational experiments are publicly available; see Alghool et al. [4] for a detailed description of the data used in the computational experiments. The data includes information about system parameters, including system capacity, fixed cost, and efficiency of the system components, namely solar collectors, PV panels, absorption chiller, compression chiller, ice chiller, ice TES, hot-water TES, cold-water TES, and auxiliary boiler. The collected data represents the year 2016. It includes hourly cooling demand and solar irradiance for Qatar over the year, as well as variable costs of producing and storing cold-water, hot-water, and electricity. As well, this paper collected additional data on the system parameters of the compression chiller, PV panels, the ice chiller, and the ice TES. They are included in Section 4 of the supplementary material. The additional data related to four system components, namely, the compression chiller, PV panels, the ice chiller, and the ice TES. For the compression and ice chiller, this paper collected data on their capacity, COP, investment cost, and the variable cost of producing a unit of cold thermal energy from them. For PV panels, this paper collected data on their fixed cost per m^2 and efficiency. For the ice TES, this paper collected data on its capacity, and investment cost.

To capture equipment sensitivity to environmental factors, this paper considers the performances of compression, absorption, and ice chillers to vary depending on outdoor temperatures. For example, a chiller performs better in cold weather than in hot weather; hence, the COP of a chiller is expected to be higher in cold weather than in hot weather. Modeling the exact relationship between the chiller's COP and outdoor temperature is complex and difficult to quantify. Therefore, this paper approximates this relationship based on a set of assumptions typically used in practice and research literature. Specifically, this paper assumes that:

- a linear relationship exists between the COP and the outdoor temperature [32],
- the maximum COP_{max} value is obtained when the outdoor temperature is at its lowest, and it is assumed to equal the given nominal COP value [28], and
- the minimum COP_{min} value is obtained when the outdoor temperature is at its highest T_{max} and it is assumed to equal to half of the nominal COP value [28].

6. Case Study and Numerical Results

The primary objective of the computational study is to assess and compare the performances of the resulting designs and operational strategies to guide managerial decision-making. Toward this goal, both STECS and HSCS are compared to other systems previously investigated in the literature, namely a Baseline Conventional Cooling System (BCCS) and the Solar Electric Cooling System (SECS). The BCCS system is a conventional cooling system that relies solely on electricity generated by power grids to operate its chillers. The SECS has a similar system structure to the BCCS, with the addition of a cold-water TES and PV panels. It also has the option of selling the surplus generated electricity to the grid to generate revenue. For brevity, this paper refers the reader to Alghool et al. [3] for details about the BCCS and SECS modeling and mathematical formulations. To ensure.

This paper consulted directly with experts in the field to ensure that problem definition, system setup, and resulting solutions are relevant and practical. This paper also conducted a comprehensive survey of related literature, as shown earlier in Section 3, to ensure that the problem assumptions, parameters, and definitions align with best practices and current market standards.

In what follows, this paper first examines the behavior of the optimized system regarding demand satisfaction. Following this, it discusses the operational performance of the cost-optimized solutions and evaluate their impact on CO_2 emissions and noise levels.

6.1. Optimized Systems Behavior: Demand Satisfaction

Tables 1–4 in Section 5 of the supplementary material provides detailed optimal solutions for the four systems. Fig. 4 illustrates the contribution of renewable and non-renewable energy sources. The main characteristics of the optimized solutions are:

- The optimized SECS met the cooling demand but relied on PV panels and the grid to meet the electricity demand. PV panels covered 57% of the demand and sold 89% of the generated electricity, generating revenue to cover 75% of the system's costs.

Table 2
Comparison of models based on operational CO_2 emissions.

System	BCCS	SECS	STECS	HSCS
Quantities of electricity supplied from grid (kWh)	15,311,750	6,427,689	N/A	12,046,053
CO_2 emissions (kg)	2,756,115	1,156,984	0	2,168,290
Rank	4	2	1	3

Table 3
Average noise level produced by various system components.

Component	Noise Level (dB)
Absorption Chiller	55
Compression Chiller	87
Ice Chiller	60
Auxiliary Electric Boiler	44

Table 4
Comparison between the four models based on noise score

System	BCCS	SECS	STECS	HSCS
Total Noise Level (dB)	87	40	27.2	54.4
Rank	4	2	1	3

- The optimized STECS had the absorption chiller meeting 83% of the cooling demand, with the remaining 17% met by the ice chiller. PV panels covered 100% of the electricity demand for the ice chiller and auxiliary electric boiler and sold 65% of the generated electricity, covering 34% of the system's costs. Solar collectors covered 84 of the hot thermal energy demand of the absorption chiller. PV panels occupied 74% of the available area, and solar collectors occupied the rest.
- The optimized HSCS had the compression chiller covering 76% of the cooling demand, while the absorption chiller covered the remaining. PV panels covered 68% of the electricity demand for the auxiliary electric boiler, and solar collectors covered 89% of the hot thermal energy demand of the absorption chiller. PV panels occupied 92% of the available area, while solar collectors occupied the rest. The system relied on non-renewable energy from the grid to meet the electricity demand for the compression chiller and auxiliary electric boiler. PV panels sold 98% of the generated electricity, generating revenue to cover 74% of the system's costs. The HSCS did not use hot-water TES in its optimal configuration.

6.2. Annual Total Net Costs

Fig. 5 compares different cooling system models based on their annual total net costs which include both the annual system costs, i.e., AIC and AOC, as well as generated revenues where applicable. It is worth noting that the BCCS is the only setup that does not generate revenues since it does not have PV panels within its configuration to generate energy and possibly sell back to the grid. In the SECS, the generated revenues help in covering 75% of the system costs. Similarly, the generated revenues in the HSCS cover 74% of the system costs. Lastly, in the STECS, the generated revenues cover 34% of the system costs. Fig. 6 provides further details on cost analysis, highlighting key differences in investment and operational costs based on the contribution of each selected system's component. As can be seen,

- The SECS model is 1.67 times cheaper than the BCCS model. Its PV panels help in fulfilling more than half of the electricity demand (57%) of the compression chiller, thus, reducing the amount of electricity withdrawn from the grid, which in turn reduces the associated cost by 138% when compared to the BCCS.
- The SECS model is 2.22 times cheaper than the STECS model. This can be explained by the smaller investment cost associated with installing SECS when compared to STECS since it operates fewer components.
- The SECS model is 9% cheaper than the HSCS model. This is due to SECS operating fewer components, which results in reduced annual investment cost when compared to HSCS, which is slightly cheaper to operate than SECS.

In summary, this paper findings show that the SECS model is the

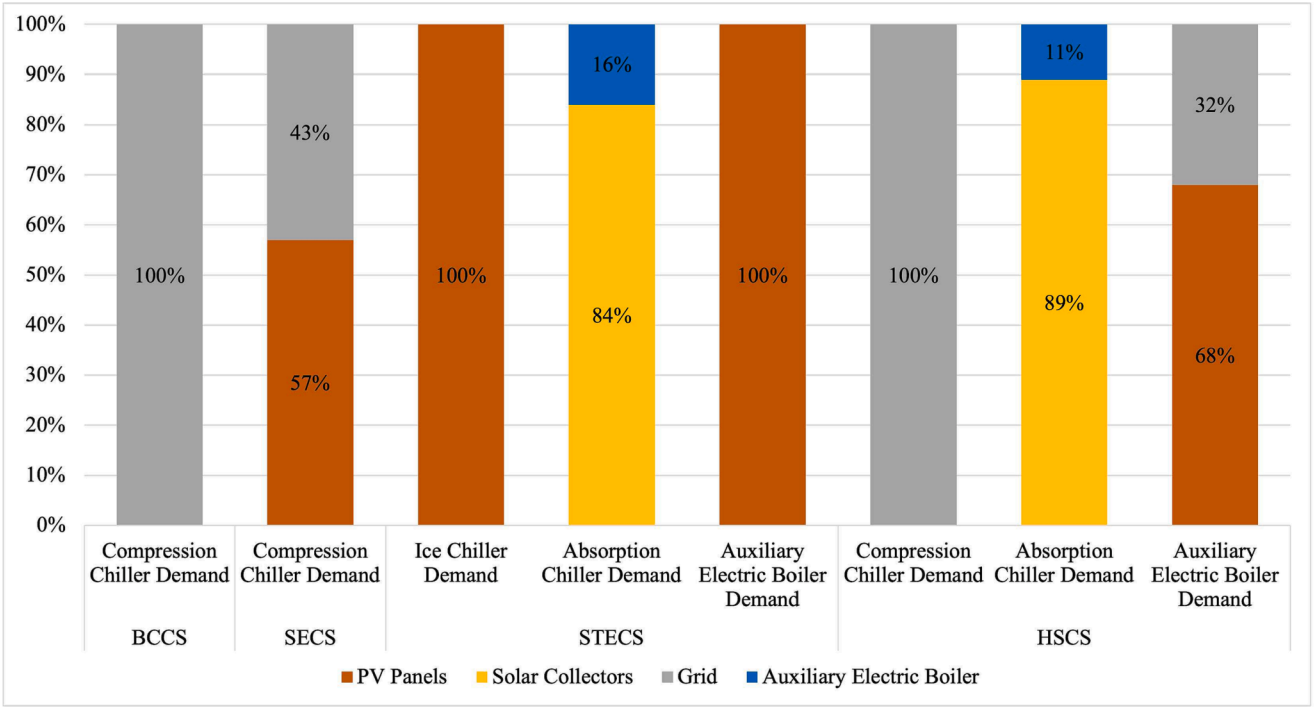

Fig. 4. Energy sources used to power system's components for demand satisfaction.

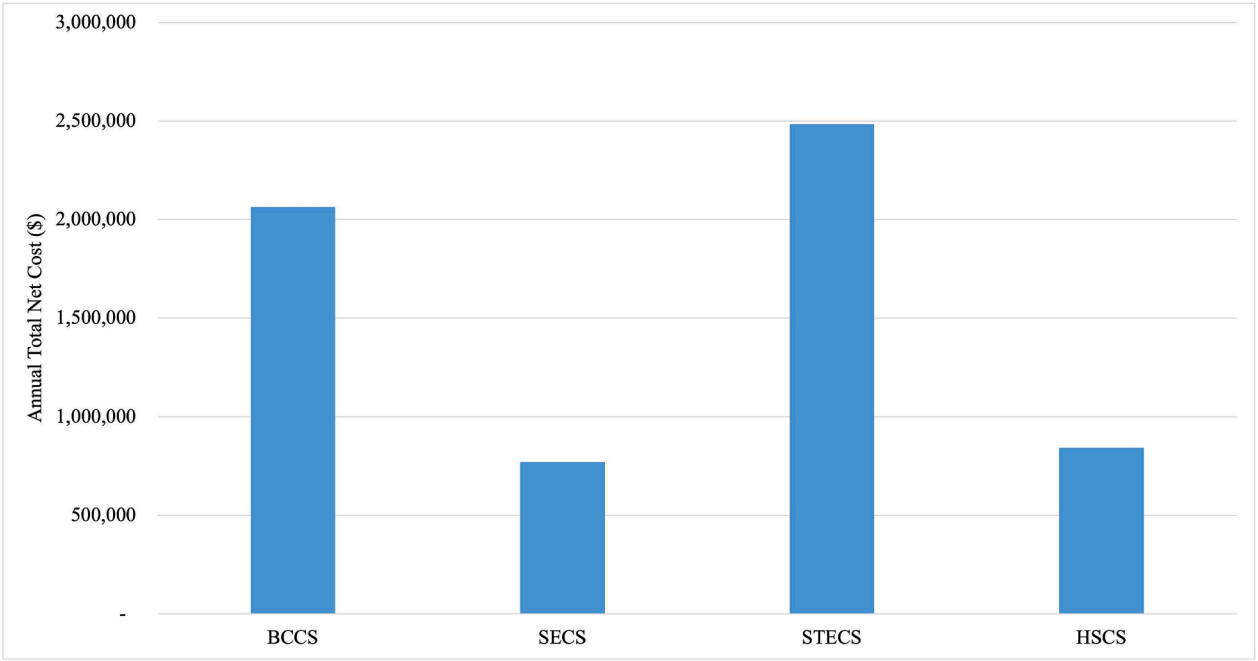

Fig. 5. Annual Total Net Costs of cooling systems.

most cost-effective in the presented case study due to its revenue generation, reduced electricity demand, and fewer components. The HSCS model, on the other hand, has a lower operational cost, but it is still more expensive overall than the SECS model.

6.3. CO_2 Emissions

This paper computed operational CO_2 emissions for each cooling system model by following the below steps:

1. The decision variables related to producing energy from compression chiller, absorption chiller, and auxiliary boiler, are calculated when the models are optimized. These components emit carbon dioxide (CO_2), because they use the electricity supplied from the grid as source of energy to produce the required thermal energy. The decision variables are energy required to produce cold thermal energy from absorption chiller (F_t^{Oab}) or compression chiller (F_t^{Oco}), and hot thermal energy from the auxiliary boiler (B_t).
2. The values of these decision variables are then multiplied by a conversion factor of 0.18 kg/kWh to estimate the quantity of CO_2

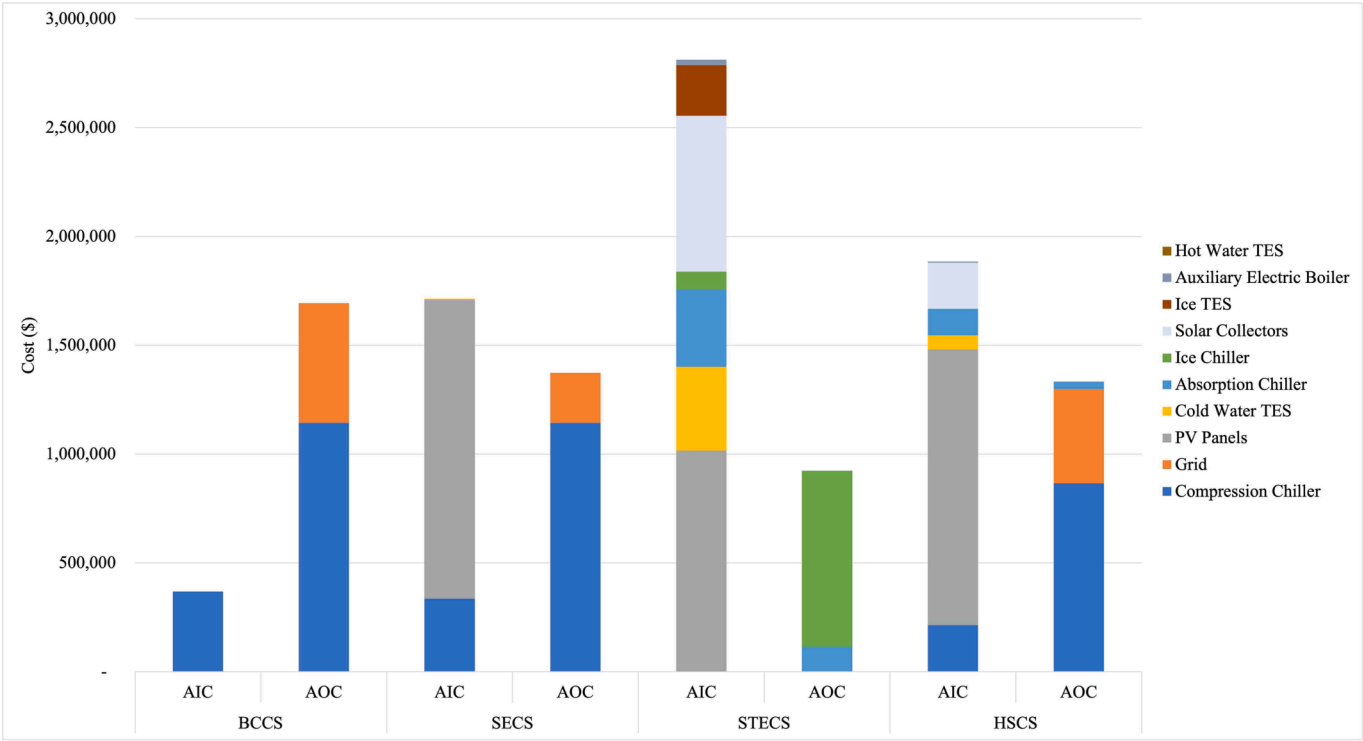

Fig. 6. Economic analysis of components of cooling systems under study.

emitted during the combustion of natural gas, the primary fuel employed in Qatar for electricity generation, to yield one kilowatt-hour of energy as found in [13].

3. The total emissions of each model is then calculated by summing the calculated CO_2 of each component over the observed period (i.e., 8784 h). For instance, for the HSCS model, the total emissions are calculated using the following equation:

$$\text{HSCS Total Emissions} = 0.18 * \left[\sum_{t\in T} F_t^{Oab} + \sum_{t\in T} F_t^{Oco} + \sum_{t\in T} F_t^{Oco} B_t\right]$$

Table 2 summarizes the results, which show that introducing renewable solar energy significantly reduces CO_2 emissions, with the STECS system emitting nearly zero. Compared to the baseline BCCS model, the SECS system reduced CO_2 emissions by 58% by satisfying 57% of the electricity demand with PV panels, and the HSCS model reduced CO_2 emissions by 21% due to the use of an absorption chiller and solar collectors. The importance of integrating solar energy into district cooling systems is highlighted as it can significantly reduce operational CO_2 emissions. Note that this analysis only covers operational emissions and not emissions through the life cycle of the components.

6.4. Noise Levels

Compression chillers can be a significant source of noise pollution in densely populated urban areas. This noise pollution can lead to serious health problems and is therefore important to consider when designing district cooling systems, particularly since they are often located in urban areas. To address this issue, a proposed method for quantifying the noise pollution generated by each model is introduced, and a noise score is calculated for each component and system. The noise score for each component is computed based on two aspects: the estimated average noise level produced by each component when it operates and the noise duration estimated by the operational time of the system's components. The noise score is calculated by multiplying the percentage of operation time of each component by its estimated noise level and then adding the noise levels of the components based on a weighted sum formula:

$$\text{System's Noise Score} = \sum_{i\in I} n_i p_i,$$

where i is the component index, n_i is the component's noise level, and p_i is the percentage of operation time of the component. Table 3 illustrates the estimated noise levels of each component when it operates [26,30,20,29], and Table 4 summarizes the comparison results obtained from the models based on the calculated noise scores during the observed periods. This paper observes that the baseline BCCS has the highest noise score among the other models, which is 87 dB. In contrast, the STECS has the lowest noise score, which is 27.2 dB, since it employs an ice chiller with a lower noise level than compression chillers, and does not operate for long periods in the system. It is important to note that noise scores can be significantly reduced when renewable energy is introduced into systems in the form of solar energy. When comparing the baseline BCCS with other systems, the noise scores have decreased by 54% for the SECS, 69% for the STCES, and 37% for the HSCS. This highlights the significance of integrating solar energy in district cooling systems to reduce noise levels.

7. Multi-criteria Assessment

This section addresses the paper's second fold of the problem. It first summarizes the ranks of the optimized models based on the three assessment criteria independently. It employs Shannon's entropy and TOPSIS methods to find the best system while considering the three criteria which are:

- Annualized investment and operating costs. As the expected revenue is the same for all cooling systems, minimizing fixed and variable costs is crucial for profitability and return on investment. It is measured in U.S. dollars.

Table 5
Summary of the four alternatives ranking

Alternatives	BCCS	SECS	STECS	HSCS
Annual Total Net Costs	3	1	4	2
CO_2 Emissions	4	2	1	3
Noise Level	4	2	1	3

Table 6
The calculated objective weights of the criteria

Criteria	Weight
Annual Total Net Cost	0.219
CO_2 Emissions	0.621
Noise Level	0.160

- Annual CO_2 emissions resulting from cooling system operation. Reducing emissions is paramount, given the global focus on transitioning to a decarbonized economy. It is measured in kg.
- Noise level. Conventional compression chillers are known to generate noise, making their placement in densely populated urban areas challenging. Minimizing noise levels enhances social acceptance. It is measured in dB.

7.1. General Model Ranking

Table 5 shows the ranks of the four models based on the three assessment criteria: the annual total net cost, CO_2 emissions, and noise levels. The results show that when considering the annual total net cost criterion only, the SECS achieves the best performance compared to the other systems. For the CO_2 emissions criterion, the STECS achieves the best performance. The same is true when considering the noise level criterion.

7.2. TOPSIS Model Ranking

TOPSIS method is used as a multi-criteria analysis approach to select the best system based on multiple criteria. First, the Shannon entropy method is used to find the objective weights of the criteria. After that, the TOPSIS method is used to assess the system based on the three criteria simultaneously.

Step 1: This paper uses the Shannon entropy method to find the objective weights of the criteria.

Table 6 summarizes the results obtained from the Shannon entropy method which represents the calculated objective weights of the criteria. The objective weights are used as input to TOPSIS.

From the Shannon entropy method, the CO_2 emissions criterion has the highest weight with 0.621, while the noise level criterion has the least weight at around 0.160.

Step 2: This paper uses TOPSIS to assess the alternatives Table 7 summarizes the results obtained from the TOPSIS method, which are the calculated performance score and rank of the alternatives.

Based on the TOPSIS analysis, it can be concluded that the STECS is the best system from a multi-criteria standpoint, as it achieves the first rank with a performance score of 0.811. This means that when considering all three criteria, which are the annual total net cost, CO_2 emissions, and noise level, the STECS achieves the best performance when compared to the other systems. The SECS, HSCS, and BCCS achieve the second, third, and fourth ranks, respectively.

Table 7
The calculated performance score and rank of the alternatives

Alternative	BCCS	SECS	STECS	HSCS
Performance Score	0.053	0.604	0.811	0.292
Rank	4	2	1	3

8. Conclusion

This paper has addressed two research questions. The first is related to designing an efficient integrated solar cooling system, namely STEC and HSCS while considering three important criteria: annual total net cost, CO_2 emissions, and noise level. To achieve this, this paper developed large-scale MILP models that aimed to determine the optimal design of system components and the optimal hourly operating policy throughout the year. To demonstrate the computational effectiveness of these models, this paper utilized real data from an educational district in Qatar. The second research question is related to performing a comparative analysis of four optimized solar cooling systems, namely BCCS, SECS, STECS, and HSCS to determine the best system when all criteria are considered simultaneously. To evaluate all criteria simultaneously, this paper employed the TOPSIS and Shannon's entropy methods.

The results of the first research question have shown that the integration of solar energy into conventional cooling systems has the potential to significantly reduce the annual total net cost by 61%, CO_2 emissions by 60%, and noise levels by 53%, on average. These findings highlight the environmental and economic benefits of incorporating solar energy into cooling systems. The results of the second research question demonstrated that SECS has the best performance in terms of the annual total net cost criterion, while STECS outperformed the others in terms of CO_2 emissions and noise levels. However, when all the criteria are considered simultaneously, the STECS, which relies entirely on solar energy, emerged as the best-performing system. On the other hand, BCCS, a conventional electricity-driven chiller, exhibited the lowest performance score, making it the least desirable option from a multi-criteria standpoint.

Moving forward, potential research extensions could focus on addressing stochasticity in demand or supply-side operations. For instance, a robust optimization approach could be employed to develop designs that are resilient to changes in demand and supply patterns for different customers utilizing various energy sources. Such an approach would enable planners to understand better the trade-offs between the desired level of system robustness and various operational measures, including costs and service levels.

Declaration of Competing Interest

The authors declare that they have no known competing financial interests or personal relationships that could have appeared to influence the work reported in this paper.

Data availability

The data are available in Alghool et al. (2020a) and in the Supplementary Material

Acknowledgement

The authors would like to thank Dr. Samer Fikry, Professor of Mechanical Engineering from the Mechanical and Industrial Engineering department at Qatar University, for sharing his extensive expertise in cooling technologies.

Open Access funding provided by the Qatar National Library.

Appendix A. Supplementary data

Supplementary data associated with this article can be found, in the online version, at https://doi.org/10.1016/j.ecmx.2024.100530.

References

[1] Abdollahi G, Sayyaadi H. Application of the multi-objective optimization and risk analysis for the sizing of a residential small-scale cchp system. Energy Build 2013; 60:330–44.
[2] Abusaibaa GY, Al-Aasam AB, Al-Waeli AH, Al-Fatlawi AWA, Sopian K. Performance analysis of solar absorption cooling systems in iraq. Int J Renew Energy Res 2020; 10(1):223–30.
[3] Alghool D, ElMekkawy T, Haouari M, Elomri A. Optimal design and operation of conventional, solar electric, and solar thermal district cooling systems. Energy Sci Eng 2022;10(2):324–39.
[4] Alghool D, Elmekkawy T, Haouari M, Elomri A. Data of the design of solar assisted district cooling systems. Data in Brief 2020;30:105541.
[5] Al-Noaimi F, Khir R, Haouari M. Optimal design of a district cooling grid: Structure, technology integration, and operation. Eng Optim 2019;51(1):160–83.
[6] Al-Ugla A, El-Shaarawi M, Said S, Al-Qutub A. Techno-economic analysis of solar-assisted air-conditioning systems for commercial buildings in Saudi Arabia. Renew Sustain Energy Rev 2016;54:1301–10.
[7] Ayadi O, Al-Dahidi S. Comparison of solar thermal and solar electric space heating and cooling systems for buildings in different climatic regions. Sol Energy 2019; 188:545–60.
[8] Bilardo M, Ferrara M, Fabrizio E. Performance assessment and optimization of a solar cooling system to satisfy renewable energy ratio (rer) requirements in multi-family buildings. Renewable Energy 2020;155:990–1008.
[9] Brandoni C, Renzi M. Optimal sizing of hybrid solar micro-chp systems for the household sector. Appl Therm Eng 2015;75:896–907.
[10] Brumana G, Franchini G, Ghirardi E. Performance assessment of solar cooling systems with energy storage. E3S Web of Conferences 2021;312:08014.
[11] Calise F, Libertini L, Vicidomini M. Design and optimization of a novel solar cooling system for combined cycle power plants. J Cleaner Prod 2017;161: 1385–403.
[12] Eicker U, Colmenar-Santos A, Teran L, Cotrado M, Borge-Diez D. Economic evaluation of solar thermal and photovoltaic cooling systems through simulation in different climatic conditions: An analysis in three different cities in europe. Energy Build 2014;70:207–23.
[13] EPA. (2014). Emission factors for greenhouse gas inventories. https://www.epa.gov/sites/default/files/2015-07/documents/emission-factors_2014.pdf.
[14] Fumo N, Bortone V, Zambrano JC. Comparative analysis of solar thermal cooling and solar photovoltaic cooling systems. J Sol Energy Eng 2012;135(2). https://doi.org/10.1115/1.4007935.
[15] Gang W, Augenbroe G, Wang S, Fan C, Xiao F. An uncertainty-based design optimization method for district cooling systems. Energy 2016;102:516–27.
[16] Khan MS, Badar AW, Talha T, Khan MW, Butt FS. Configuration based modeling and performance analysis of single effect solar absorption cooling system in trnsys. Energy Convers Manage 2018;157:351–63. https://doi.org/10.1016/j.enconman.2017.12.024.
[17] Khir R, Haouari M. Optimization models for a single-plant district cooling system. Eur J Oper Res 2015;247(2):648–58.
[18] Noro M, Lazzarin R. Solar cooling between thermal and photovoltaic: An energy and economic comparative study in the mediterranean conditions. Energy 2014; 73:453–64.
[19] Otanicar T, Taylor RA, Phelan PE. Prospects for solar cooling–an economic and environmental assessment. Sol Energy 2012;86(5):1287–99.
[20] Packaged Glycol chiller. (2021). https://www.pattonnz.com/downloads?category=technical-brochures.
[21] Papoutsis E, Koronaki I, Papaefthimiou V. Numerical simulation and parametric study of different types of solar cooling systems under mediterranean climatic conditions. Energy Build 2017;138:601–11.
[22] Porumb R, Porumb B, Bălan M. Baseline evaluation of potential to use solar radiation in air conditioning applications. Energy Procedia 2016;85:442–51.
[23] Reda AM, Ali AHH, Morsy MG, Taha IS. Design optimization of a residential scale solar driven adsorption cooling system in upper egypt based. Energy Build 2016; 130:843–56.
[24] Shirazi A, Taylor RA, White SD, Morrison GL. Transient simulation and parametric study of solar-assisted heating and cooling absorption systems: An energetic, economic and environmental (3e) assessment. Renewable Energy 2016;86:955–71.
[25] Sokhansefat T, Mohammadi D, Kasaeian A, Mahmoudi A. Simulation and parametric study of a 5-ton solar absorption cooling system in tehran. Energy Convers Manage 2017;148:339–51.
[26] Sound data and application guide for air-cooled series rtm chiller. (2017). https://www.tranehk.com/files/Products/RTAGPRB001AEN_1117.pdf.
[27] Soussi M, Balghouthi M, Guizani A, Bouden C. Model performance assessment and experimental analysis of a solar assisted cooling system. Sol Energy 2017;143: 43–62.
[28] Thu K, Saththasivam J, Saha BB, Chua KJ, Murthy SS, Ng KC. Experimental investigation of a mechanical vapour compression chiller at elevated chilled water temperatures. Appl Therm Eng 2017;123:226–33.
[29] Vaillant specification boiler range. (2018). https://www.vaillant.co.uk/downloads/specification-1/vaillant-specification-boiler-bro-2018-aw-1-0-15-web-1733495.pdf.
[30] Vamtec. (2018). Vamtec: Yazaki hot water absorption chiller - 17kw to 352kw cooling from waste heat. https://www.vamtec.com/absorption-chiller/.
[31] Wang J, Qi X, Ren F, Zhang G, Wang J. Optimal design of hybrid combined cooling, heating and power systems considering the uncertainties of load demands and renewable energy sources. J Cleaner Prod 2021;281:125357.
[32] Welcome to kensa heat pumps. (2022).https://www.kensaheatpumps.com/.
[33] WMO. (2021). Greenhouse gas bulletin: Another year another record. https://public.wmo.int/en/media/press-release/greenhouse-gas-bulletin-another-year-another-record.
[34] Zeng J, Li Z, Peng Z. Exergoeconomic analysis and optimization of solar assisted hybrid cooling systems in full working conditions. Appl Therm Eng 2022;206: 118082.
[35] Zhang J, Li Z, Jing Y, Xu Y. Performance of solar absorption-subcooled compression hybrid cooling system for different flow rates of hot water. Appl Sci 2020;10(3):810.